Journal of Rehabilitation Research
and Development Vol. 30 No. 4, 1993
Pages 393-404

A Technical Report

A closed loop automated seating system

Richard J. Kwiatkowski, MS and Rafael M. Iñigo, PhD
Department of Electrical Engineering, University of Virginia, Charlottesville, VA 22903

Abstract—This technical report presents the recent progress in the design and construction of a closed loop automated seating system. Preliminary test results are reported. The system is designed to measure seating surface forces and control the seating surface geometry of a seated human. It uses force information as feedback to determine custom seating contours which produce desired seating characteristics. Ultimately, the system is intended to be used for research studies with patients.

The system consists of an electronically actuated, force-sensing seating surface which is controlled by a computer. Stepper motors are used to move force sensing probes up or down until the desired seating surface characteristic is attained.

Preliminary test results are presented and analyzed. A force-equalizing control algorithm has been written and found to produce relatively uniform force distributions for soft, hemispherical loads of various weights.

Key words: *cushion, force feedback, force sensor, seat contours, seating, skin ulcer, wheelchair.*

INTRODUCTION

Wheelchair users who spend many hours sitting are at risk of developing pressure sores. Factors that affect the cause of pressure sores may include the magnitudes, directions, and durations of applied external pressures as well as tissue properties including: temperature, moisture, tissue viability, age, and hygiene (1,2). In the hope of preventing pressure sores, wheelchair users often utilize custom contoured cushions. In this report, custom contoured cushions are defined as foam cushions that have been manufactured or modified for use by a specific individual in order to distribute the tissue/support interface pressures as desired. A popular method of characterizing a seating surface is to measure the resultant interface pressures. Some of the problems associated with this technique are: 1) it may be hard to distinguish high, but safe pressures from high, but harmful ones; 2) it is not known exactly what a "safe" pressure may be for a given individual; 3) normal interface pressure measurements alone do not account for potentially damaging shear or frictional forces; and, 4) the presence of the measurement device at the tissue/support interface may modify the quantity to be measured (3). The quantitative comparison of the undeformed, unloaded shape of the buttocks to the loaded one has been suggested to be a better method of measuring the net effect of the external load (3). A review of the literature reveals that a purely hydrostatic loading condition in which the external pressures are uniform and the tissue deformation is minimized may be an optimal seating situation (3,4). Studies have been taken which have shown that the use of custom contoured cushions can result in lower mean interface pressures and more uniformly distributed pressures than those resulting from noncontoured cushions (5,6,7).

Due to the potential benefits of using custom contoured cushions, products have been designed to aid in the measurement and fabrication of such cushions (8,9,10,11). However, there exist few tools

Address all correspondence and requests for reprints to: Richard J. Kwiatkowski, Thornton Hall, Department of Electrical Engineering, University of Virginia, Charlottesville, VA 22903.

Journal of Rehabilitation Research and Development Vol. 30 No. 4 1993

which allow for simultaneous adjustment of contours and measurement of the resulting interfacial forces. The seating system described in this paper will have these capabilities. This system will reduce the amount of wasted time and materials which result from trial-and-error-based adjustments to custom cushions, because the trial-and-error process occurs while a client is seated on the system before the cushion is ever fabricated.

The Closed-Loop Automated Seating System (CLASS) described in this paper is meant to be used in conjunction with the Custom Cushion Fabrication System (CCFS) designed at the University of Virginia Rehabilitation Engineering Center (UVA REC) (11,12); however, its applicability could easily be extended to other fabrication techniques. A typical cushion could conceivably be designed with the use of the CLASS and then fabricated with the CCFS, all within an hour, and produce high quality contouring with minimal wasted material. The CLASS could be a useful tool to assess different seating contours and their resulting load distributions.

METHODS

System Design Specifications

The system described in this paper has evolved over the last five years and is the result of the efforts of various researchers who have worked on the project at the UVA REC (11,12,13,14,15). Some of the desired specifications for the system are listed below:

1. The system should be able to measure seated individuals with masses up to 100 kg. This value is the same as the International Standards Organization (ISO) maximum wheelchair test dummy mass.
2. The controllable seating surface area should be no less than 45.7 cm by 45.7 cm.
3. Each probe should be capable of measuring static forces normal to the seated surface ranging from 20 to 5900 grams with a resolution of at least 33.2 grams.
4. The actuator linear position resolution should be better than ± 0.78 millimeters.
5. The system convergence time should be no longer than 5 minutes.

These specifications were chosen to ensure that the system would be able to measure 95 percent of the potential subjects as well as to ensure that the displacement and force resolutions are as good as, or better than, existing systems.

System Overview

Figure 1 illustrates the main components of the CLASS. The seating surface consists of an 11×12 rectangular array (minus the four corner elements) of movable force sensing probes. The system uses motor-driven actuators which can position each probe vertically within a 12.7 cm range with a ± 0.1mm vertical resolution. Since 128 motors are required (one for each probe), the size of the motors is an important consideration. The stepper motors chosen are small enough to allow two layers of 64 motors to fit in the available area and powerful enough to lift the rated 5900 gram load when coupled with acme drive screws. Also, the stepper motors allow the position of a given probe to be calculated from the number of pulses sent to the respective motor, if steps are not missed. This eliminates the need for separate position sensors for each probe.

The probes are connected to a control system via cables and interfacing circuitry. The system contains an STD bus multiple processor computer with its related input/output and user interfacing equipment. Multiple processors allow for a controller hierarchy in which a host processor runs high

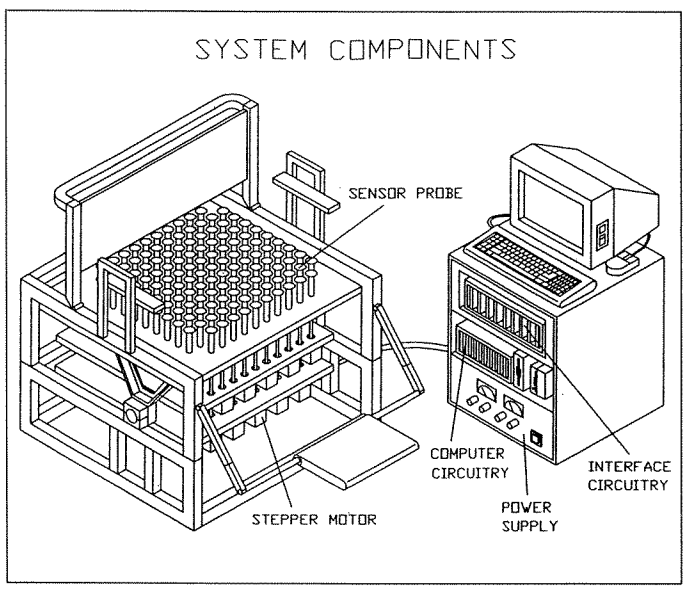

Figure 1.
Closed Loop Automated Seating System components.

level tasks and monitors three peripheral processors which independently and concurrently control either the probe actuator or force sensing signals. The system contains a monitor, keyboard, and mouse for user interaction. It also contains a D.C. power supply which is used for energizing the stepper motors, the force transducers, and the orientation potentiometers, as well as the supporting circuitry. Attached to the chair unit, analog multiplexers are used to scan the force and orientation signals before they are digitized and sent to the computer. Also located on the chair unit are controller cards that receive digital signals from the computer and convert them into the drive pulses for the stepper motors.

The chair body can be adjusted to simulate the client's wheelchair (or stationary chair). The seating surface and chair back can be independently tilted to the front and back. The arm and foot rests can also be adjusted to support the client as desired.

System Information Flow

A description of how information flows through the CLASS is given below. Referring to **Figure 2**, we see that the system can be represented by a closed-loop block diagram. The forward path starts on the left with the desired seating characteristics. This represents the information entered by the system operator regarding the desired features of the resulting seating contour. This information may be

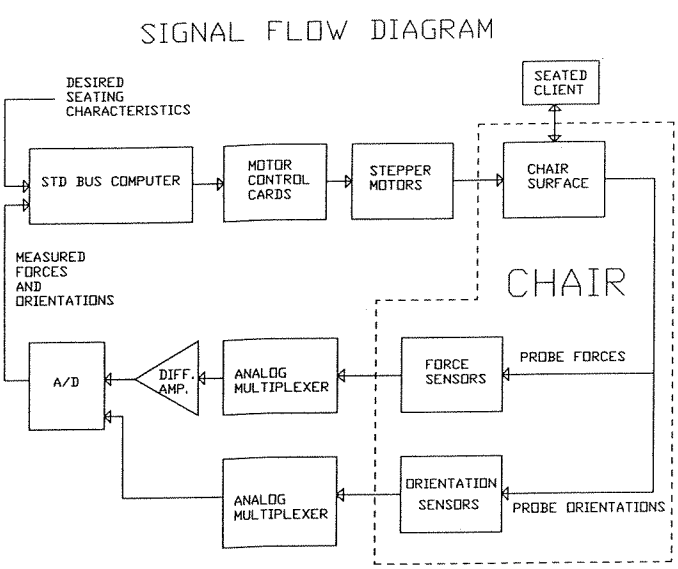

Figure 2.
Signal flow diagram of system.

the desired force distribution (uniform, inversely proportional to stiffness, minimal specific site pressures, etc), or other features specific to a given client. This information is sent to the host STD bus computer via a keyboard or file indicating force distribution preferences. The computer analyzes this information and the current probe force and orientation signals and, by running a selected contour algorithm, determines the new probe position adjustments. Drive signals are sent to the stepper motor control cards where they are converted into the stepper pulses and sent to the motors. The stepper motors are coupled to acme drive screws which transform the rotary motion into the vertical probe positions. The load (the body of the seated individual) reacts to the probe adjustments, and the probe heads tilt and rotate with the new load position.

The feedback path of the block diagram consists of the probe force and orientation signals produced by the force and orientation sensors. The force sensors convert the vertical forces along the probe axes into voltage signals which are scanned, amplified, and sent to an analog-to-digital converter (A/D) to be digitized. The scanned orientation sensors' outputs are in the range of from 0 to 5 volts and are therefore not amplified before being digitized. The A/D then serializes the force and orientation signals and sends them to the host computer via an RS-232 serial link where the feedback path is completed. The host computer program then examines this new information and determines if the desired seating characteristics are met. If they are, the process is completed and the final seating parameters (probe positions, forces, etc.) are saved. If the desired characteristics are still not met, the process continues as described above.

Force Sensor

To measure the force normal to a given probe head, it is necessary to determine the three-dimensional surface normal vector. This is done by measuring the orientation of the probe head as well as the vertical component of the force acting on the probe. Potentiometers are used to measure the orientation angles of the probe head, and a cantilever beam strain gage force sensor is used to measure the vertical force acting on the probe. **Figure 3** shows a detailed view of three probes positioned at different heights. A cross-sectional drawing of a typical probe is shown in **Figure 4**.

Journal of Rehabilitation Research and Development Vol. 30 No. 4 1993

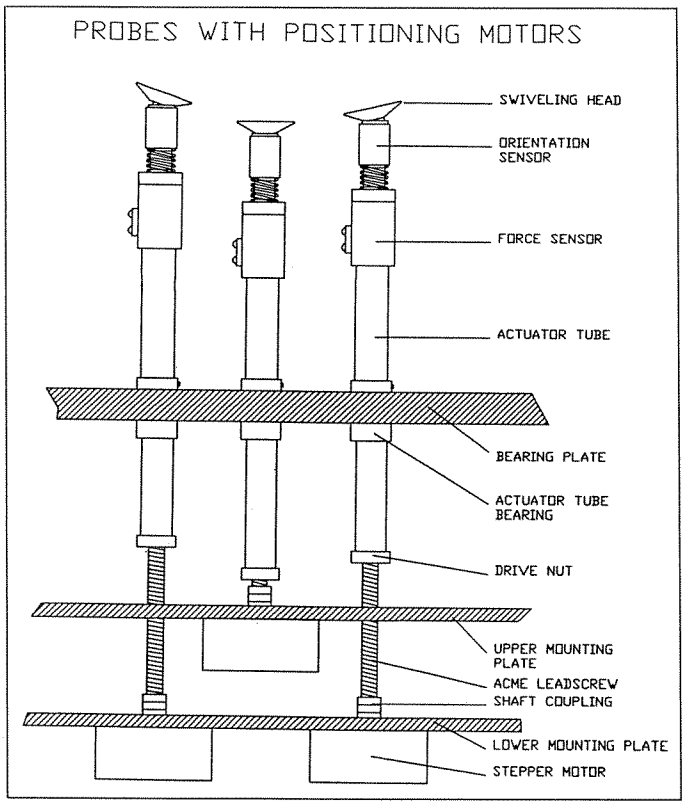

Figure 3.
Side view of three motor-actuated, force-sensing probes.

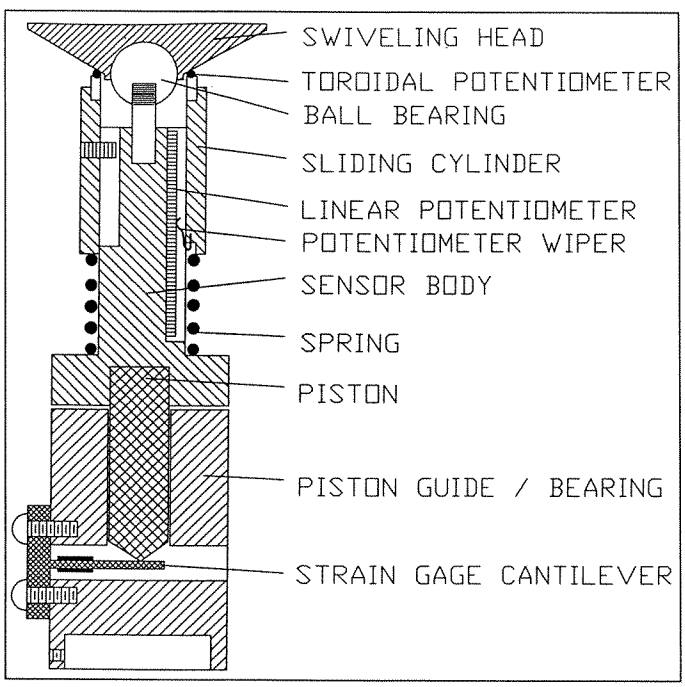

Figure 4.
Cross-sectional view of a typical force-sensing probe.

The force sensor consists of four strain gages wired in a "full resistive bridge" network. It is possible to use fewer gages to measure the applied load, but the full bridge offers linearity, temperature compensation, maximum sensitivity, and increased noise immunity due to the differential output. The vertical force applied to the probe is transmitted down a steel piston to the cantilever beam. The piston has a conical end where it comes in contact with the cantilever beam to concentrate the load at approximately one point. An overload safety feature has been designed into the probe by allowing only a specific amount of deflection in the beam to occur before the sensor body comes in contact with the piston bearing. This deflection is set by adjusting the cantilever beam vertically with the use of two mounting screws and slotted holes in the vertical portion of the beam.

Each probe surface consists of a conical swiveling head which tilts and rotates freely with the seated surface by means of a ball and socket joint (see **Figure 4**). The orientation of the probe head is detected by two separate potentiometers which measure the tilt and rotation angles. The potentiometers convert the associated angles to electrical signals which are processed by the computer. The probe head can rotate freely 360° about the center axis of the connecting shaft. A toroidal potentiometer attached to the top of a sliding cylindrical collar measures the contacting point of the conical probe head, thereby determining the head rotation. This potentiometer measures the full 360° rotation minus a contact angle of about 16°.

The tilt angle of the head is measured with a separate potentiometer. The sliding collar is spring loaded and resists the tilt of the head. A wiper attached to the collar makes contact with a linear potentiometer mounted on the probe body. As the probe head tilts, the collar is forced to slide down the probe body, causing the wiper to travel along the linear potentiometer.

The tilt angle, θ, of a given probe is used to determine the force normal to the probe surface. The vertical force, F_V, acting on the probe is measured with the force sensor. The normal-to-surface force, F_N, can then be calculated using:

$$F_N = \frac{F_V}{\cos\theta}$$

where θ varies between $\pm 50°$ and has a value of zero degrees for a horizontal probe surface. This

equation assumes that the forces acting on the probe surface can be represented solely by F_N, a force located in the center of the probe head and acting normal to the surface. It is assumed that any shear forces acting along the probe surface are small compared to the normal forces and can be ignored. If necessary, the shear forces could be taken into account by determining the frictional coefficient at the seating interface.

Force Sensor Tests

The graph in **Figure 5** shows the amplified output voltage of a typical force sensor when loads from 0–6300 grams were applied in a vertical direction on the probe head. A nonswiveling probe head was used to support the load during the test. The output is fairly linear over a load range of 0–3600 grams (0–8 lbs), and then saturates for higher loads due to the overload protection built into the sensor. These data were used to calibrate the probe force sensor so that the system's computer could later calculate the load applied to the sensor. **Figure 6** shows the resulting measured vs. applied load characteristic of a typical probe when loads from 0–5400 grams were applied to the sensor. Various masses were stacked on top of each other, one at a time, then removed, one at a time, during the test to illustrate the hysteresis and the overall accuracy of the force sensor.

Tests were also taken to measure the accuracy of the force sensor when off-axis loads were applied. It was found that frictional effects acting on the surface of the piston and guide/bearing increased with tilt angle and resulted in decreased transducer accuracy. It was found that producing a vibration by moving the probe down then up 5 mm helped reduce this static friction, or "stiction," and increased the sensor's accuracy to off-axis load measurements.

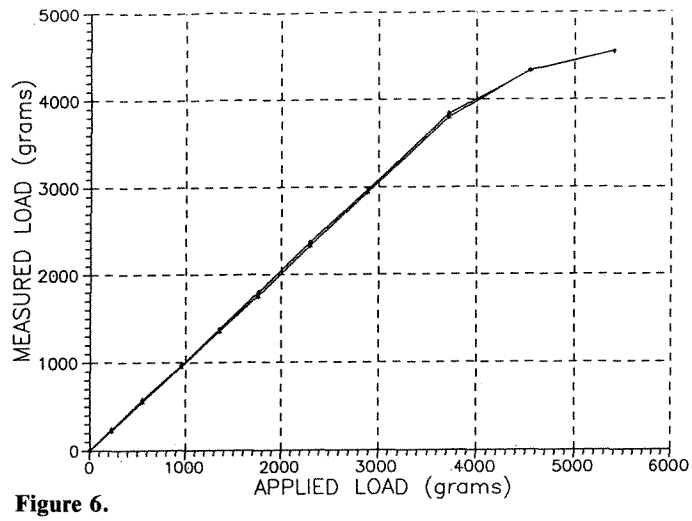

Figure 6.
Hysteresis test for vertical static loading of typical force sensor.

Orientation Sensor Tests

After the tilt and rotation sensors were calibrated, data were taken to test the accuracy of the sensors. The measured versus applied tilt and rotation angles are shown in **Figure 7** and **Figure 8**. The tilt angle data were taken by incrementally rotating the swiveling head from −50 to +50 degrees

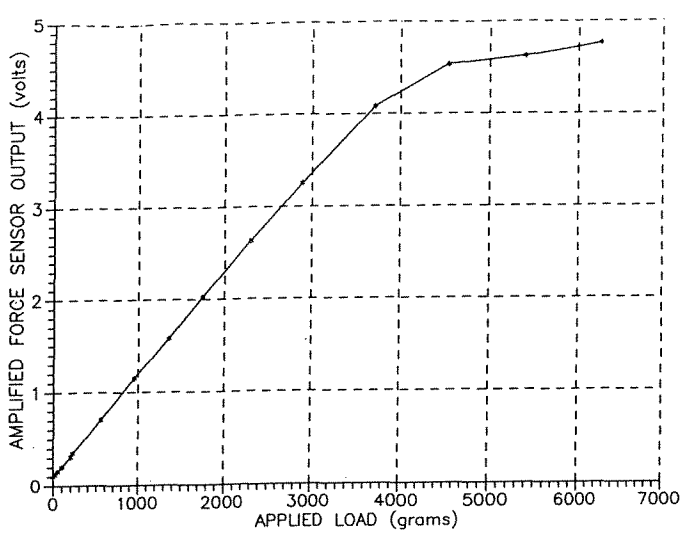

Figure 5.
Load/Voltage characteristic of typical force sensor.

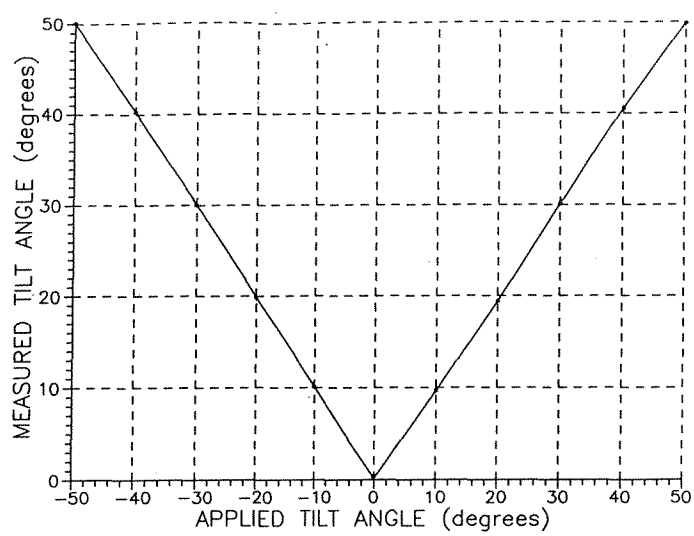

Figure 7.
Typical tilt sensor measured vs. applied angle.

Journal of Rehabilitation Research and Development Vol. 30 No. 4 1993

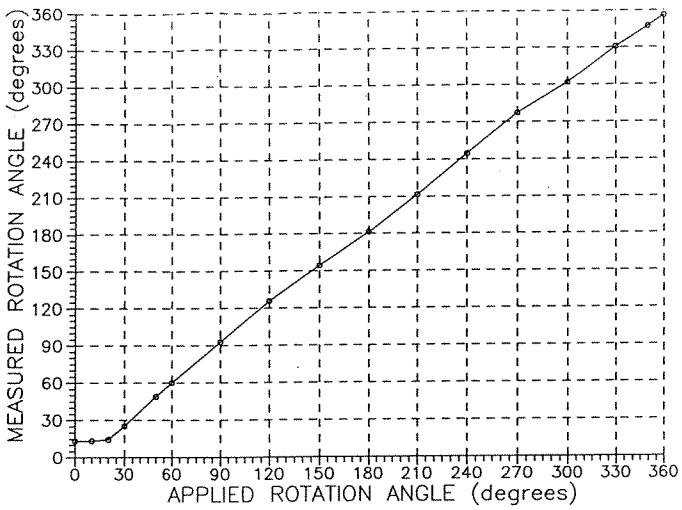

Figure 8.
Typical rotation sensor measured vs. applied angle.

through an arbitrary horizontal axis of the ball of the joint. Only the magnitude of the tilt angle is measured with the linear potentiometer. The calibrated tilt sensors were found to be accurate to within 4 percent and to have a 0.4° digital resolution.

The rotation angle data were found by fixing the tilt angle at 45° and incrementally rotating the swivelling head from 0° to 360° through the vertical axis of the ball of the joint. **Figure 8** reveals that the typical rotation sensor is inaccurate for angles between 0° and 16°. This is due to the construction of the rotation sensor toroidal potentiometer. The solder attachment of the potentiometer wire to a lead wire shorts the potentiometer which produces a zero volt output when the swiveling head comes in contact with the potentiometer within this region. For rotation angles between 16° and 360°, the sensors were accurate to within 7° and had a digital resolution of 1.5°.

Test Set-up

Sixteen probes arranged in a 4×4 array were used to test the contour algorithms. Successful completion of these tests will indicate the feasibility of complete system implementation. To avoid problems associated with load instability, the test load was supported externally from the seating surface so it could not become statically unstable and tip over. Stability problems will most likely need to be addressed when the full 128-probe seating array is tested. The load used for the test was a convex hemispherical indentor made from a rubber and glycerine gel. The indentor was chosen as a test load since it fairly realistically models the area of the human buttocks around an ischial tuberosity. In the center of the gel is a wooden core which models a bony prominence. The indentor has a diameter of 17 cm and, along with a supporting rod, weighs approximately 2900 grams. Weights can be added to the test load to increase the total weight if desired. A supporting frame was used for the tests, which kept the indentor from tilting, but allowed it to move vertically with the supporting probes. A detailed drawing of the hemispherical test load and a view of the test set-up used for the contour algorithms described below are shown in **Figure 9** and **Figure 10**.

Spring Probe Simulation Algorithm

After the test load was lowered onto the flat array surface, a quick, one-step initial contouring algorithm was used to better distribute the weight of the load. The initial algorithm is based on the CONTOUR1 algorithm described by Gordon (14). The idea is to model each probe as a spring with a stiffness k. Then, after the normal surface force, f_i, on the ith probe has been calculated, the displacement of each probe, d_i, is calculated using the spring equation:

$$d_i = \frac{f_i}{k}$$

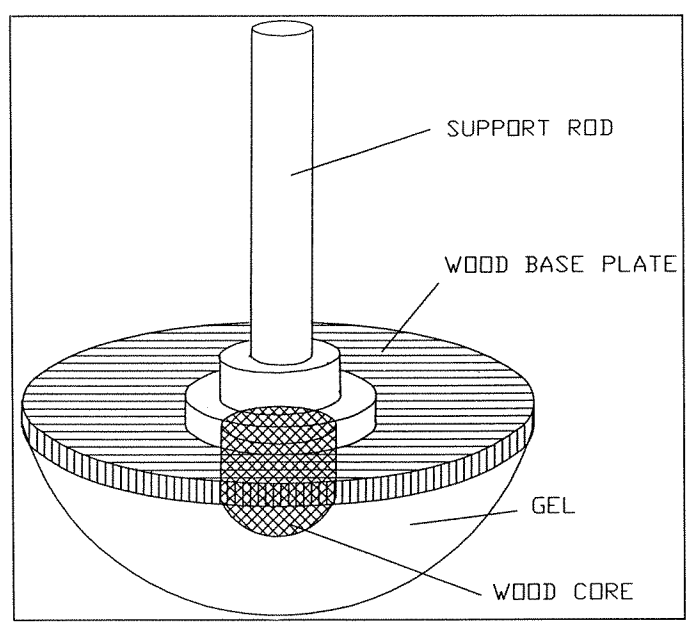

Figure 9.
Hemispherical gel test load detail.

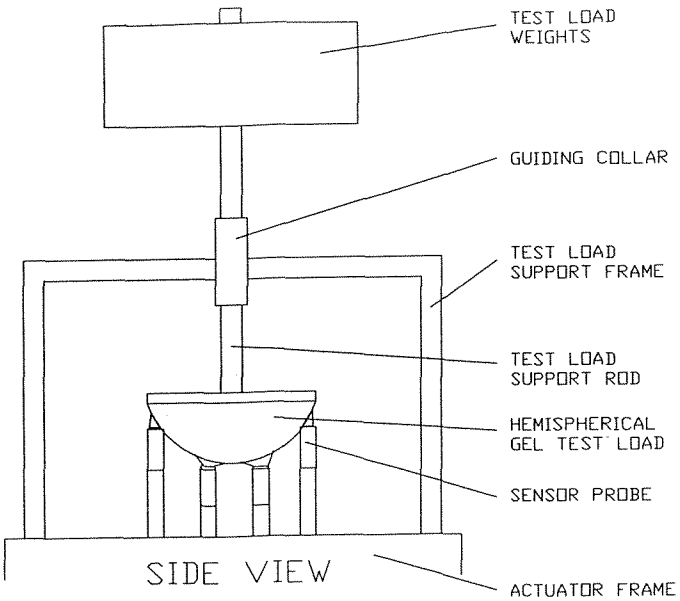

Figure 10.
Test load support frame with 4×4 probe array side view.

The probes are lowered one after another in 2.5 mm increments until they arrive at the calculated position. This process is only performed once, so it is guaranteed to end (if the process is repeated multiple times, the probe positions are not guaranteed to converge to a specific value since the force values are discrete and the force feedback is disabled during the probe motion). How well the force is distributed over the 16 probes depends on factors such as the spring stiffness k and the original weight distribution. If k is too small, then it is likely that the originally higher weighted probes will be lowered too far and, as a result, the majority of the load will be supported by the other probes. If k is too high, then the higher weighted probes will not be lowered as much, and they will end up still supporting a disproportionately large amount of the load. Unfortunately, depending on the physical characteristics of the load (i.e., the stiffness of the buttocks at various sites), it may be likely that one k is good for one type of load, and another k for a different load. So if only one spring stiffness k is used, one should not expect the load to be distributed equally well after the routine is performed for different loads.

After the spring simulation routine was run, it was found that there were still large differences between the resulting maximum and minimum probe loadings, and the following algorithm was used to equalize the probe loadings.

Force Equalizing Algorithm

The force equalizing algorithm used is based on Gordon's CONTOUR3 algorithm (14), which he found to be fairly successful at distributing loads amongst a 1×8 array. The idea behind the algorithm is to model the portion of the load supported by a probe as a spring with a stiffness K_i which is not coupled to any other part of the whole load. This stiffness can be determined experimentally by dividing the change in probe loading it experienced by the known vertical displacement it made. For relatively small displacements, this stiffness calculation can be used to decide how a probe should be adjusted so that it supports its share of the total load.

After the simulated spring algorithm has been run, the number of probes, n, in contact with the load are counted and the individual probe loadings, L_i, are summed to get the total weight. The desired probe loading, D_L, is then calculated by dividing the total weight by the number of loaded probes:

$$D_L = \frac{\sum_{i=1}^{n} L_i}{n}.$$

The vertical displacement, V_i, of a given probe is then calculated by subtracting the present loading of the probe from the calculated desired loading and dividing the result by the current stiffness value, K_i, of that portion of the load supported by the probe:

$$V_i = \frac{D_L - L_i}{K_i}.$$

The stiffness values are computed using:

$$K_i = \left| \frac{L_i - L_i^*}{V_i} \right|$$

where L^*_i is the load on the ith probe from the previous iteration of the algorithm. A flow diagram of the contouring algorithm is presented in **Figure 11**.

RESULTS

The motor-actuated, force-sensing seating probes have been designed and tested and found to accurately position loads up to 5900 g in a vertical

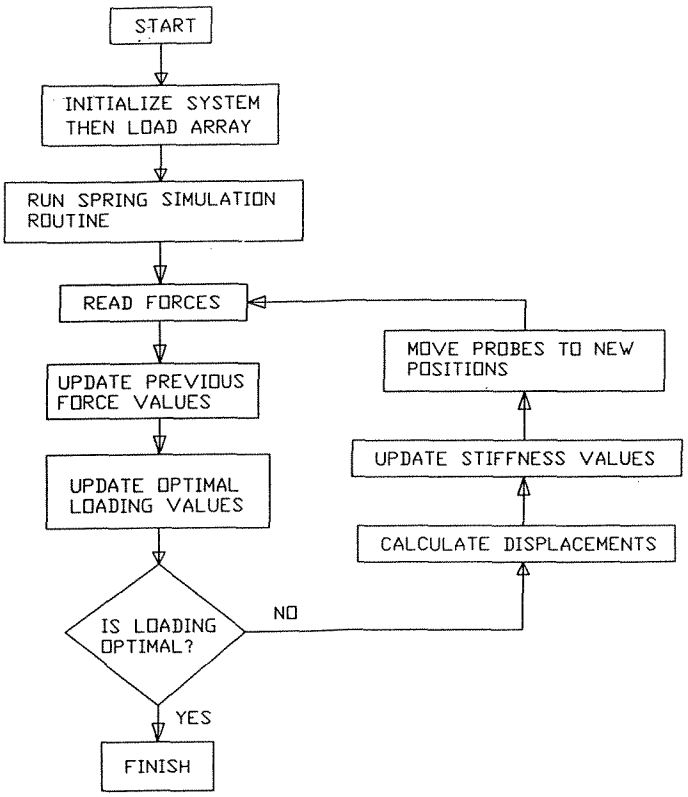

Figure 11.
Force equalizing contouring algorithm flow diagram.

range of 0–12.7 cm with a ± 0.1mm accuracy. The force sensor in each probe has been found to measure vertically applied loads from 0–4500 g with 24 g resolution and a 5 percent error when the probe is jogged up and down by 5 mm before the load is measured. The accuracy decreases for higher loads due to the nonlinear sensor behavior when the overload protection is activated. The accuracy also decreases due to friction for off-axis applied loads. The 4500 g upper limit represents a 24.2 kPa maximum pressure measurement due to the 4.26 cm probe spacing.

The hemispherical test load weighted to three different values, (2.9, 6.1, and 12.4 kg), was used to test the force equalizing algorithm. For each test, the stiffness value, k, used in the spring simulation routine was set to 50 grams/mm.

Initially, the test was run on the 2.9 kg load, and it was found that one or more of the four corner probes could come in contact with the wooden base of the test load. When this occurred, the probe(s) in contact with the very stiff wooden base would cycle back and forth during successive iterations of the algorithm. When they were in contact with the base, they tended to support too much load, and when they were lowered a little, they were not in contact with the load at all. So it was discovered that the algorithm would only converge if the probes were in contact with relatively soft loads.

Foam disks were mounted onto the test load at the areas where the corner probes had made contact with the wooden base and the algorithm was run and experimentally found to converge for all three test loads.

The algorithm was run for each of the three loads until the final probe loads were within ± 35 grams of D_L, and it took 10, 21, and 37 iterations respectively for the 2.9-, 6.1-, and 12.4-kg loads. The spring simulation procedure took an average of 33 seconds, and the force equalizing routine had an average of 16 seconds per iteration which produced total convergence times of 192, 368, and 624 seconds for the three loads. **Figures 12, 13,** and **14** show measured probe loads versus time for the three test loads with the ± 35 gram convergence criterion. Data from typical corner, edge, and center probes in the array are provided.

The probe loadings before and after the routine was run as well as the final probe displacements* for the three ± 35 gram convergence tests are shown in **Tables 1, 2,** and **3.** As can be seen from data in these tables, the final displacements for the 16 probes were not the same for the three different load weights. Since the same contour was used, but weighted to different amounts, it might seem likely that the final positions of the probes should be nearly equivalent for the three tests. This idea is based on the theory that the peak pressure between a ball and a spherical seat will be minimal when the radii are equal (16). So it may be reasonable to assume that the peak probe load will be minimized when the probe array contour is the same as that of the undeformed hemispherical load. However, the theory is only valid when the seat and ball have the same material properties (elastic and isotropic), which for these tests, they did not. Also, the undeformed load contour was not perfectly symmetrical and no attempt was made at the start of the testing to ensure that the load was placed in the same position on the probes for each test. Inaccura-

* For comparison purposes, the probe displacements have been shifted so that the probe with the highest final position has a displacement of zero.

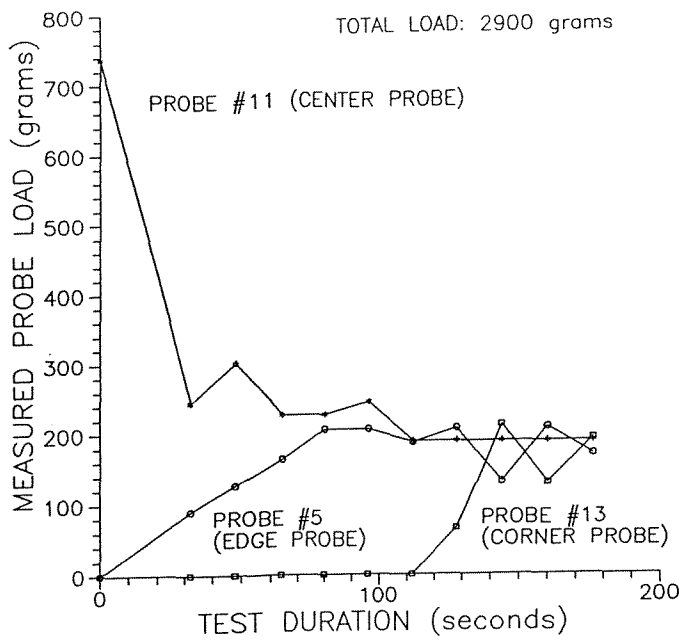

Figure 12.
Measured probe load vs. test time (2.9 kg load).

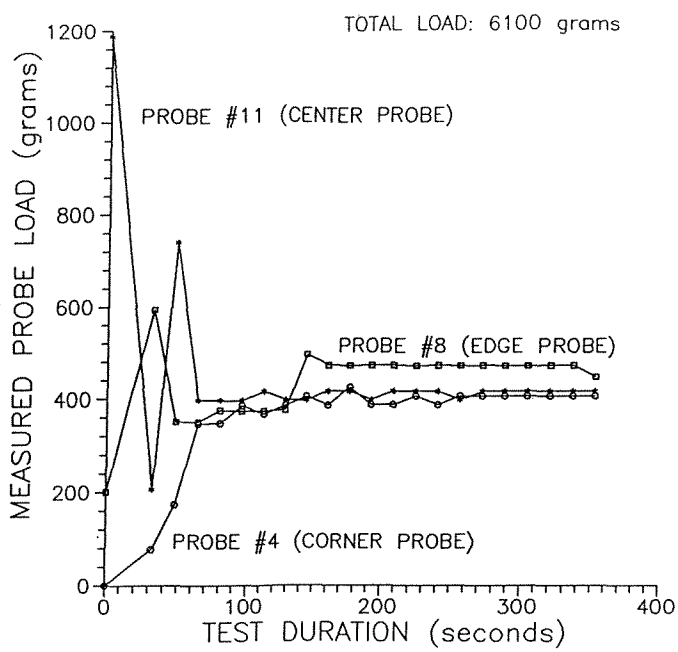

Figure 13.
Measured probe load vs. test time (6.1 kg load).

cies in the force sensors, especially for the probes with large tilt angles, may also explain the resulting differences in displacements.

The total load values measured by summing the individual probe vertical loads during each iteration are shown in **Figure 15** for the three ± 35 gram convergence tests. It was found that initially the

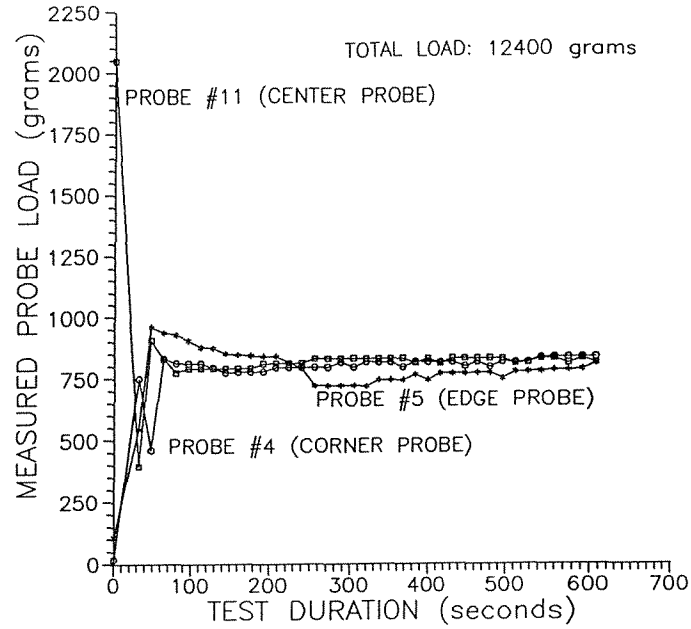

Figure 14.
Measured probe load vs. test time (12.4 kg load).

measured total loads were below actual but ended up much closer to the actual total loads with errors of 1.0 percent, -2.9 percent, and -3.8 percent, respectively for the increasing loads.

DISCUSSION

The force equalizing algorithm discussed above works well for the test load, but will need to be modified when the full 128-probe seating system is tested. The test load was supported so that it could not tip over, no matter how the probes were positioned. When a person is seated on the full system, it will be necessary to take into consideration the center of mass and the overall position of the person to make sure that (s)he is not being positioned in an unstable, or other undesirable manner.

Another issue not mentioned so far has to do with the load-bearing ability of specific sites on the seated individual. Obviously, certain areas are more suited to supporting the weight of the body than others. Also, to help reduce pressure sores, it may be better to more heavily load thick-tissued, low-stiffness areas of the buttocks than thin-tissued, stiff areas which are close to bones. There may also be specific sites which should not be heavily loaded for

Table 1.
Force equalizing routine run data (2.9 kg load).

Initial Probe Loads (grams)				Final Probe Loads (grams)				Final Probe Displacements (mm)			
0	0	0	0	174	186	206	184	13.1	19.6	18.3	12.2
0	902	737	0	197	213	189	178	18.4	36.8	35.0	14.9
0	596	433	0	174	186	177	185	17.9	33.9	33.5	15.3
0	0	0	0	182	170	190	192	4.5	9.7	8.9	0.0

Ideal probe load based on summed normal loads: 186.4 grams.

Table 2.
Force equalizing routine run data (6.1 kg load).

Initial Probe Loads (grams)				Final Probe Loads (grams)				Final Probe Displacements (mm)			
0	201	135	0	406	447	435	406	7.7	21.7	23.1	14.4
151	1443	1188	78	439	418	416	413	20.3	40.2	37.6	18.4
58	956	823	21	409	413	415	392	17.2	35.0	35.0	15.6
0	18	0	0	381	412	415	426	2.2	10.4	11.0	0.0

Ideal probe load based on summed normal loads: 415.2 grams.

Table 3.
Force equalizing routine run data (12.4 kg load).

Initial Probe Loads (grams)				Final Probe Loads (grams)				Final Probe Displacements (mm)			
19	510	353	41	837	834	835	821	6.7	19.1	23.1	10.9
474	2257	2048	254	821	827	813	824	20.8	37.4	35.4	17.3
254	1457	1349	264	824	836	826	823	15.9	33.6	32.3	16.3
0	109	141	0	816	810	826	828	0.0	8.4	10.3	2.4

Ideal probe load based on summed normal loads: 825.1 grams.

other reasons such as the presence of pressure sores, bruises, cuts, etc.

To accomplish these objectives, it is necessary for the algorithm to have some knowledge of which parts of the body are loading specific probes as well as their relative supporting ability. The overall orientation of the body on the system can be partially controlled by the operator and assisting personnel. If there are specific low-load capability sites known, these could be entered into the computer by the operator and used as boundary conditions in the contouring algorithm.

Brienza's contouring algorithm (12) allowed for different criteria for determining the optimal probe loadings. Although he came up with a solution for a specific case: loadings which were inversely proportional to the load stiffness for a 2×4 array, his algorithm could theoretically be solved for the whole 11×12 array and use other performance criteria.

The maximum load that can be accurately measured with the force sensor could possibly be increased by adjusting the overload protection gap. An increase in the thickness of the strain gage aluminum beam would allow for larger loads to be measured. The hysteresis errors measured for the off-axis loads are mainly due to the friction present between the sensor piston and guide bearing. This friction could be reduced with a better bearing

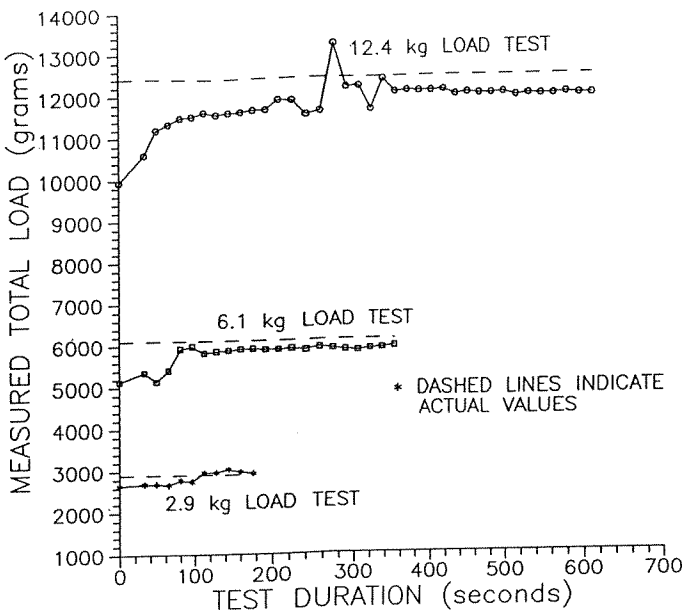

Figure 15.
Measured total load vs. test time.

design possibly incorporating ball bearings or other materials. Overall, the current force sensor has the best balance between sensitivity, accuracy, and maximum load measuring capability of the various sensors designed and tested by the CLASS researchers to date.

A force-equalizing contouring algorithm was tested on a 4×4 subsection of the whole seating array, and the typical convergence times were longer than 5 minutes for the heavier two loads tested. During the tests, only one probe was moved at a time, and the probe positioning time was the limiting factor in the overall test duration. It seems likely that the convergence time will increase approximately linearly with more probes. To keep the total time to near 5 minutes for the full 128 probes, it may be necessary to modify the stepper motor controller circuitry to allow up to 16 motors to be moved at once. Other algorithms can and will be implemented to satisfy more sophisticated seating contour criteria once the system is fully operational.

No attempt has been made at this point to prove that the force-equalizing algorithm will converge for all (or even any) loads. Preliminary testing has suggested that the system has trouble converging with very stiff loads but consistently converges for relatively soft loads. Since the human buttocks are generally relatively soft, this is encouraging; however, some theoretical work should be made to show what types of conditions are required for the algorithm to converge.

CONCLUSION

The CLASS has been designed to determine seating contour/load relationships for individuals with masses up 100 kg. The controllable seating surface dimension is 50.4 cm by 46.2 cm, which should be large enough to seat approximately 95 percent of the intended individuals with special seating needs. A 4×4 portion of the whole array has been tested and found to be capable of producing contours which result in fairly uniform force distributions for a soft hemispherical load. The seating system when completed should be a useful tool for investigating the effects of seating contours on the resulting load distributions. It should be possible to determine contours that produce fairly uniform force distributions, thereby approximating hydrostatic loading conditions which produce minimal tissue distortion.

ACKNOWLEDGMENTS

Funding for this research was provided by NIDRR grant H133E80003 and in part by both the Potomac Edison Company and Virginia Power.

REFERENCES

1. Bennett L, Kavner D, Lee BK, Trainor FA. Shear vs pressure as causative factors in skin blood flow occlusion. Arch Phys Med Rehabil 1979:60:309-14.
2. Krouskop TA. A synthesis of the factors that contribute to pressure sore formation. Med Hypotheses 1983:11:255-67.
3. Levine SP, Kett RL, Ferguson-Pell M. Tissue shape and deformation versus pressure as a characterization of the seating interface. Assist Technol 1990:2:93-9.
4. Chow WW, Odell EI. Deformations and stresses in soft body tissues of a sitting person. J Biomech Eng 1978:100:79-87.
5. Chung KC, DiNello AM, McLaurin CA. Comparative evaluation of pressure distribution on flat foams and contoured cushions. In: Proceedings of the 10th Annual RESNA Conference, 1987 June; San Jose, CA. Washington, DC: RESNA Press, 1987:323-5.

6. Sprigle S, Faisant T, Chung KC. Clinical evaluation of custom-contoured cushions for the spinal cord injured. Arch Phys Med Rehabil 1990:71:655-8.
7. Sprigle S, Chung KC, Brubaker C. Reduction of sitting pressures with custom contoured cushions. J Rehabil Res Dev 1990:27(2):135-40.
8. Welter RJ, Zysman S. Three dimensional machining of custom contoured polyethylene foam cushions. In: Proceedings of the 10th Annual RESNA Conference, 1987 June; San Jose, CA. Washington, DC: RESNA Press, 1987:576-8.
9. Neth DC, McGovern TF, Reger SI. Computer aided measurement and fabrication of contoured body supports. In: Proceedings of the 12th Annual RESNA Conference, 1989 June; New Orleans, LA, Washington, DC: RESNA Press, 1989:234-5.
10. Chung KC, McLaurin CA, Brubaker CE, Brienza DM, Sposato BA. A computer-aided shape sensing system for custom seat contours. In: Proceedings of the 13th Annual RESNA Conference, 1990 June; Washington, DC: RESNA Press, 1990:395-6.
11. Brienza DM, Chung KC, Brubaker CE. Computer design and fabrication of custom-contoured seating. Med Design Mater 1991:Jan:32-41.
12. Brienza DM. Seat contour optimization using force feedback (Dissertation). Charlottesville, VA: University of Virginia, 1991.
13. Malinowski JL. Automated contouring of a wheelchair seating support. Charlottesville, VA: University of Virginia, Engineering Report. 1987.
14. Gordon JR. Control algorithms and mechanical components for an automatic body contour measurement system (Thesis). Charlottesville, VA: University of Virginia, 1989.
15. Kwiatkowski RJ, Inigo RM. The design of a computer aided seating system. In: Proceedings of RESNA International '92, 1992 June; Toronto, Ontario, Washington, DC: RESNA Press, 1992:216-8.
16. Timoshenko SP, Goodier JN. Theory of elasticity. 3rd ed., New York: McGraw-Hill, 1970.